A Numerical Model of ISAR Distortion and an Efficient Procedure for Restoring Distorted ISAR Images

S. Wong, E. Riseborough and G. Duff
Defence R&D Canada – Ottawa
3701 Carling Ave. Ottawa, Ontario, Canada K1A 0Z4

silvester.wong@drdc-rddc.gc.ca

ABSTRACT

Distortion in the ISAR image of a target is known to cause by non-uniform rotational motion of the target during image formation. The conventional explanation describes the image distortion as a quadratic phase distortion effect. This quadratic phase distortion effect is significant only when the target image is integrated over an extended period of time; i.e., over a large angular rotation by the target. In many measured ISAR images such as those from in-flight aircraft, the distortion can be quite severe; but the image integration time is only a few seconds in duration and the target's relative rotational displacement is only a few degrees at the most. Quadratic phase distortion is not adequate in explaining the severe blurring in many of these observations. Furthermore, time-frequency analysis of the distorted images often reveals that the Doppler frequency of the target is fluctuating randomly in nature and displays no quadratic phase behaviour temporally. A numerical model based on a time-varying target rotation rate has been developed to model the observed distortion. It has successfully modelled the severe distortion with all the observed characteristics. The model's simulated results have been validated by experimental data. The severe distortion is attributed to the phase modulation effect where a time-varying Doppler frequency provides the smearing mechanism. It has been shown that the quadratic phase distortion can be considered as a special case of the phase modulation effect. The distortion in ISAR images can be refocused by signal processing techniques. Time-frequency methods, in particular, are quite effective in refocusing distorted (or blurred) ISAR images. In time-frequency processing, an ISAR image of a target is extracted at a particular instant of time; a focused image is thus obtained because the target's motion can be considered as relatively uniform over a short duration. However, there are a large number of time instants to deal with in time-frequency processing. It is impractical to examine all refocused ISAR images to search for the best images. An efficient ISAR refocusing procedure has been developed. An optimum refocused image can be obtained quickly without having to process systematically a large number refocused ISAR images. Examples of refocused ISAR images are given using measured data.

1.0 INTRODUCTION

Inverse Synthetic Aperture Radar (ISAR) imaging provides a 2-dimensional radar image of a target. A 2-dimensional picture can potentially offer crucial distinctive information about the features of the target that can lead to more accurate target identification in Non-Cooperative Target Recognition application. An ISAR image is generated from the target's rotational motion. This motion can sometimes be quite complex, such as the motion of a fast, maneuvering jet aircraft. As a result, severe distortion can occur in the ISAR image of the target [1]. An illustration is shown in Figure 1. Two ISAR images of an in-flight aircraft were taken in a consecutive sequence in time. The image on the left (a) is severely blurred; the image on the right (b) is well

Paper presented at the RTO SET Symposium on "Target Identification and Recognition Using RF Systems", held in Oslo, Norway, 11-13 October 2004, and published in RTO-MP-SET-080.

focused. It has been recognized that a time-varying perturbed motion in the rotation of the target is responsible for the image blurring [2]. Figures 2a and 2b show the azimuth displacements of the same aircraft in Figure 1 as a function of time as recorded independently by a ground-truth instrument mounted on-board of the aircraft. In addition, the temporal phase history of a scattering centre on the aircraft for both the blurred and focused ISAR images also display the same behaviour as the azimuthal motion of the aircraft; this is illustrated in Figures 2c and 2d. It can be seen clearly that there is a direct correspondence between the distortion in the ISAR image and the temporal motion of the target.

Conventional ISAR model attributes the ISAR image distortion to a quadratic phase effect. This quadratic phase is a consequence of a circular motion of target with respect to the radar, resulting in a non-constant Doppler velocity introduced along the radar's line of sight due to acceleration of the target from the circular motion [3]. Quadratic phase distortion does not provide an adequate account of the severe blurring in many of the observations from real targets. Furthermore, time-frequency analysis of the distorted ISAR images often reveals that the motion of the target is fluctuating randomly in nature and displays no quadratic temporal behaviour. In order to obtain a better understanding of the severe distortion in ISAR images, we have developed a numerical model that is based on a time-varying target rotational motion. It will be shown that this model provides a very accurate representation of the distorting mechanism. The model links the distortion phenomenon to a phase modulation effect in the returned radar echo from the target.

In this paper, a description of the ISAR distortion model based on the phase modulation effect will be presented. It will be shown that the quadratic phase distortion can be seen as a special case of phase modulation. An experiment is set up to study the ISAR distortion. Controlled experiments are performed to demonstrate the severe distortion. The experimental data are used to compare and validate the model's simulated results, showing that the phase modulation effect is a reasonable model. An efficient procedure has also been developed, based on the insights gained from the modelling work, to allow a distorted image to be restored quickly. The restoration of distorted ISAR images is relevant and useful in target recognition applications that exploit ISAR imagery.

2.0 ISAR DISTORTION EXPERIMENTS

An ISAR experiment is designed and set up to examine distortion in ISAR images due to time-varying rotational motion. There are a number of reasons why data from a controlled experiment are desirable. In a controlled experiment, the locations of the scattering centres of the target are known precisely and the rotational motion of the target can be programmed to produce the effects that are sought for analysis. Moreover, experiments of a given set of conditions can be repeated to verify the consistency of the results. These are not always possible with real target such as an aircraft.

A delta-wing shaped apparatus, the Target Motion Simulator (TMS), has been built for the ISAR distortion experiments. A picture of the TMS target is shown in Figure 3. The target measures 5 m on each of its three sides. Six trihedral reflectors are mounted on the TMS as scattering centres of the target. A time-varying rotational motion can be introduced by a programmable motor drive. ISAR images of the TMS are collected using a stepped frequency radar waveform at X-band (8.9 GHz to 9.4 GHz). Figure 4 shows a schematic of the experimental set-up. A sequence of ISAR images of the TMS apparatus are shown in Figure 5 as the target makes a transition from a constant rotation to a time-varying rotational motion. The ISAR image is well focused with the 6 reflectors shown clearly when the target is rotating with a constant motion of about 2.0 degrees/s; this is illustrated in Figure 5a. The ISAR images then become distorted when a fluctuating motion is added to the motion of the target as seen in Figures 5b and 5c. This fluctuating motion is shown in Figure 6 and is extracted from the distorted ISAR using time-frequency method [5].

3.0 ISAR DISTORTION MODEL

A numerical model has been developed to simulate the distorting effect of a multi-scatterer target. To simplify the problem, we will consider just one scatterer on the target in describing the model to bring out the basic mechanism more clearly without any loss of generality. The phase of the radar return signal from a scatterer on a moving target is given by,

$$\phi = \frac{4\pi f}{c}\left(R - vt - X(t)\right) \tag{1}$$

where f is the transmitting radar frequency, R is the initial distance of the scatterer on the target from the radar at the on-set of the radar imaging scan, v is the radial velocity of the target and $X(t)$ is the displacement due to the rotation of the target along the radar's line of sight. For simplicity, we consider either a stationary target or perfect translational motion compensation; i.e., v is set to zero. In other words, we focus only on the rotational aspect of the target in forming the ISAR image. Moreover, we assume the rotational axis of the target is perpendicular to the radar line of sight to simplify the geometry.

Consider a scatterer on a 2-dimensional target with a pair of coordinates (x_0 , y_0) with respect to the target's rotational axis. This is shown in Figure 7. A change in the scatterer's coordinates due to rotation at a later time t is given by

$$\begin{pmatrix} x(t) \\ y(t) \end{pmatrix} = \begin{pmatrix} \cos(\omega(t)\,t) & -\sin(\omega(t)\,t) \\ \sin(\omega(t)\,t) & \cos(\omega(t)\,t) \end{pmatrix} \begin{pmatrix} x_0 \\ y_0 \end{pmatrix} \tag{2}$$

Hence, the displacement along the radar's line of sight $X(t) = x(t) - x_0$ due to a rotation of the target is given by

$$X(t) = \left(x_0 \cos(\omega(t)\,t) - y_0 \sin(\omega(t)\,t) \right) - x_0 \tag{3}$$

A fluctuating motion can be described, in general, by a Fourier series; i.e.,

$$\omega(t) = \omega_0 + \sum_{n=1}^{\infty} \left(a_n \sin(2\pi\Omega_n t) + b_n \cos(2\pi\Omega_n t) \right) \tag{4}$$

where ω_0 is the constant rotational rate of the target in the absence of any extraneous fluctuating motion, a_n , b_n and Ω_n can be considered as the random variables for fitting $\omega(t)$ to any fluctuating motion.

An ISAR image is generated using a sequence of HRR profiles. The HRR profile of a scatterer is given by [4],

$$H_n = A_n \exp\left(j \frac{4\pi f_c}{c} (R - X(t)) \right) \tag{5}$$

where A_n is the amplitude of the HRR profile , n is the range-bin index, f_c is the center frequency of the radar bandwidth. R and $X(t)$ are defined in Equation (1). A Fourier transform is performed at each of the range bins over the sequence of HRR profiles to generate an ISAR image; i.e.,

$$I_{n,m} = \sum_{k=0}^{M-1} A_{n,k} \exp\left(j \frac{4\pi f_c}{c} (R - X(t)) \right) \exp\left(j \frac{2\pi}{M} mk \right) \tag{6}$$

where m is the cross-range bin index, $m = 0, \ldots, M\text{-}1$. M is the number of HRR profiles used in the generation of the ISAR image. Effectively, the Fourier transform converts the HRR variable at each range bin from the time domain into the frequency domain. Hence, the cross-range axis of the ISAR image represents the Doppler frequency as observed by the radar. The term that is of interest in the analysis of the ISAR image is the factor containing the temporal rotational motion in Equation (6); i.e.,

$$\begin{aligned} \psi(t) &= \exp\left(-j \frac{4\pi f_c}{c} X(t) \right) \\ &= \exp\left[-j \frac{4\pi f_c}{c} \left(x_0 \cos(\omega(t)t) - y_0 \sin(\omega(t)t) \right) - x_0 \right] \end{aligned} \tag{7}$$

where $X(t) = x(t) - x_0$ is the change in range of the scatterer with respect to the radar along the radar's line of sight. Normally, the ISAR image of a target is captured during a relatively small rotation of the target; for example, the ISAR images generated in Figure 1 correspond to a rotation of about 3 degrees, as indicated in Figure 2. Thus, a small rotation approximation can be assumed (i.e., $\omega(t)t << 1$), to simplify the mathematical description. This helps to bring out the phase modulation effect a bit more clearly. Equation (7) then becomes

$$\psi(t) = \exp\left[-j \frac{4\pi f_c}{c} \left(x_0 \frac{(\omega(t)t)^2}{2} - y_0 \omega(t) t \right) \right] \tag{8}$$

It can be seen from Equation (8) there are two components that affect the phase due to a time-varying rotation, a first order term, $\omega(t)t$ and a second order term $(\omega(t)t)^2$. A further simplifying step is made by considering a time-varying rotational rate,

$$\omega(t) = \omega_0 + \omega_r \sin(2\pi\Omega t) \tag{9}$$

where ω_r is the rotational amplitude of the fluctuating motion and is a function of Ω, the oscillation frequency of the time-varying motion. This is equivalent to taking the first two terms of the Fourier series as given in Equation (4).

Consider a time instant when the scatterer is located $(0, y_0)$, the scatterer's motion is parallel to the radar's line of sight; see Figure (7). Thus this will have the largest Doppler effect as seen by the radar. Substituting Equation (9) into Equation (8),

$$\begin{aligned} \psi(t) &= \exp\left[+j \frac{4\pi f_c}{c} y_0 \left(\omega_0 + \omega_r \sin(2\pi\Omega t)t \right) \right] \\ &= \exp\left[+j \frac{4\pi f_c}{c} y_0 \omega_0(t) t \right] \exp\left[+j \frac{4\pi f_c}{c} y_0 \omega_r \sin(2\pi\Omega t)t \right] \end{aligned} \tag{10}$$

The first factor corresponds to a constant rotation of the target. This factor provides a Doppler shift that allows the placement of the scatterer along the cross-range axis to form an undistorted ISAR image of the target in the absence of any fluctuating motion. The second factor describes the phase modulation effect due to a small fluctuating motion of the scatterer that can introduce distortion. To see how the phase modulation effect comes about more clearly, the second phase factor in Equation (10) can be rewritten as,

$$\mu(t) = \exp\left(\; j \frac{4\pi f_c}{c} y_0 \omega_r \int \sin(2\pi \Omega t) \; dt \right) \tag{11}$$

$$= \exp(-j \; k \; \sin(\eta))$$

$$= \cos(k \sin(\eta)) - j \sin(k \sin(\eta))$$

$$= (J_0(k) + 2J_2(k)\cos(2\eta) + 2J_4(k)\cos(4\eta) + \ldots)$$

$$- j(2J_1(k)\sin(\eta) + 2J_3(k)\sin(3\eta) + 2J_5(k)\sin(5\eta) + \ldots)$$

where

$$k = \frac{4\pi f_c}{c} \; y_0$$

$$\eta = \sin^{-1}\left[\; -\omega_r \int \sin(2\pi \Omega t) \, dt \; \right]$$

and the J_n are the Bessel functions of the first kind of order n. It can be seen from Equation (11) that the phase of a time-dependent rotational motion consists of many higher order sideband components. These higher order sideband components are a consequence of phase modulation arising from the fluctuating motion and they generate a smear in the image as a result.

4.0 NUMERICAL ANALYSIS OF ISAR DISTORTION

Figure 8 shows the distorted ISAR image computed by the numerical model, using the experimental time-varying target motion as shown in Figure 6 as input. The target has rotated about 8 degrees over a 4-s imaging period. It can be seen from Figure 8 that the computed distortion in the ISAR image compares quite well with that in the experimental image in Figure 5c.

A more physical description of how phase modulation leads to distortion can be seen as follows. It is well known that a scatterer will migrate along the cross-range axis in the ISAR image if the scatterer's Doppler frequency f_D is changed during the imaging period [3]. The number of cross-range bins migrated is given by,

$$K = abs\left(\frac{1}{\Delta f_D} (f_{D,t=0} - f_{D,t=T}) \right) \tag{12}$$

for a monotonically changing f_D, where Δf_D is the cross-range resolution. As a result, there will be a "smear" in the ISAR image of the scatterer along the cross-range axis when there is a change in the Doppler frequency during the imaging period. The radar line of sight Doppler frequency of a scatterer on the target will have an

oscillating behaviour due to the time-varying input that drives the target. Figure 9a shows the computed Doppler frequency of scatterer #1 from the distorted ISAR image in Figure 8. The amount of distortion generated at scatterer #1 is the same as the amount of change in the Doppler frequency; this is clearly seen in Figure 9. In this case, the amount of change in the Doppler frequency is ($f_{D,\,max}$ - $f_{D,\,min}$) over the imaging duration. This result is expected since the cross-range dimension of the ISAR image is effectively the Doppler frequency as explained in Section 2.

Note that scatterer #6 in the ISAR image in Figure 8 has hardly any distortion. It corresponds to a scatterer located at (x_0, 0); see Figure 7. The phase of scatterer #6, according to equation (8), is given by,

$$\psi(t) = \exp\left[-j \frac{4\pi f_c}{c} x_0 \frac{(\omega(t)t)^2}{2} \right] \tag{13}$$

That is, the phase is quadratic in $\omega(t)t$. The Doppler frequency of scatterer #6 is illustrated in Figure 10a. Comparing with scatterer #1 (Figure 9a), the change in the Doppler frequency of scatterer #6 is very small; hence there is no noticeable distortion. Thus, the second order term $(\omega(t)t)^2$ has negligible distorting effect compare to the first order term $\omega(t)t$ in Equation (8). To summarize briefly, a scatterer with a changing Doppler frequency due to the target's time-varying motion provides the physical basis for the large distortion in the ISAR image. The model's simulated results are validated by the experimental data, demonstrating that phase modulation provides an accurate picture of the distortion mechanism.

The conventional quadratic phase distortion effect [3] can be considered as a special case of the phase modulation effect. The quadratic phase distortion assumes a target's rotational motion is constant during the imaging period; that is, $\omega(t) = \omega_0$ in Equation (9). Any change in the Doppler frequency by any of the scatterers on the target is due to a non-linear Doppler velocity introduced along the radar's line of sight as a result of acceleration from the rotational motion. This can be seen by substituting $\omega(t) = \omega_0$ into Equation (8). The phase of the rotating scatterer becomes

$$\psi(t) = \exp\left[-j \frac{4\pi f_c}{c} \left(x_0 \frac{(\omega_0 t)^2}{2} - y_0 \omega_0 t \right) \right] \tag{14}$$

Examining a scatterer located at (0, y_0) on a target as shown in Figure 7, Equation (14) becomes,

$$\psi(t) = \exp\left[j \frac{4\pi f_c}{c} y_0 \omega_0 t \right] \tag{15}$$

That is, $\psi(t)$ is a perfect linear phase in time. Therefore, the Doppler frequency is a constant. In other words, for scatterers that have motions nearly parallel to the x-axis, their Doppler frequency will have very little change and thus there will be very little distortion according to Equation (12). For a scatterer located at (x_0, 0), Equation (14) becomes

$$\psi(t) = \exp\left[-j \frac{4\pi f_c}{c} x_0 \frac{(\omega_0 t)^2}{2} \right] \tag{16}$$

Equation (16) displays a phase with a quadratic dependence in time. Hence the Doppler frequency will be changing with time, resulting in a blur in the ISAR image according to Equation (12).

To see how much a distorting effect the quadratic phase would have on the ISAR image, a constant ω_0 value corresponds to the maximum value of the experimental rotational rate, $|\omega_{\max}| = 3.9$ deg./s as given in Figure 6, is used to run the numerical model for the TMS target. The resulting ISAR image is shown in Figure 11. The amount of distortion in the image is much less than that of the case when a time-varying rotational rate $\omega(t)$ is used. This is quite evident by comparing Figure 11 with Figure 8.

Another interesting observation that is worthy to note is that in the quadratic phase distortion case, the largest distortion occurs at scatterer #6 of the target as seen in Figure 11. The large distortion at scatterer #6 can be explained by the fact that the rate of change of the Doppler frequency is maximum for a scatterer that is located near the x-axis in a rotational motion as depicted in Figure 7. At the location (x_0 , 0) and using Equation (2), the movement of scatterer #6 parallel to the x-axis is given by

$$x(t) = x_0 \cos(\omega_0 t) \tag{17}$$

Its velocity parallel to the x-axis is

$$v_x = \frac{dx(t)}{dt} = -x_0 \omega_0 \sin(\omega_0 t) \tag{18}$$

Hence, $v_x = 0$ at the initial position (x_0, 0) and time $t = 0$. The velocity of scatterer #6 is perpendicular to the x-axis. This is intuitively obvious as shown in Figure 7. However, the rate of change of v_x

$$\frac{dv_x}{dt} = -x_0 \omega_0^2 \cos(\omega_0 t) \tag{19}$$

is maximum at (x_0, 0) because $\cos(\omega_0 t) = 1$ at $t = 0$.This implies that the Doppler frequency of scatterer #6 has the largest change along the x-axis; therefore a large distortion occurs as a result.

To illustrate the quadratic phase distortion's dependence on $(\omega_0 t)^2$, the ISAR image in Figure 11 is generated using a generously large ω_0 value; i.e., $\omega_0 = 3.9$ degrees/s. This corresponds to a target rotation of 15.6 degrees over a 4-second imaging time. In the time-varying rotating case (Figure 8), the target rotation is only 8.2 degrees over the 4-second duration. Using a ω_0 value corresponds to a target rotation of 8 degrees, the quadratic phase case is computed again using a lower ω_0 value of 2 degrees/s. The resulting ISAR image of the target is shown in Figure 12. It can be seen that none of the scatterers on the target shows any distortion in the image, even scatterer #6 which should display the most distortion. This result is consistent with the experimental ISAR image shown in Figure 5, where scatterer #6 displays no noticeable distortion. In summary, it is seen from the above analysis that the quadratic phase distortion effect is not adequate for describing the ISAR distortion that is seen in the experimental images. The quadratic phase effect is a second order effect (i.e,. $(\omega_0 t)^2$) and it produces a much smaller distortion than that from the phase modulation effect.

5.0 RESTORATION OF DISTORTED ISAR IMAGES

For target recognition applications, ISAR images of targets must have adequate spatial resolution. According to the principles of ISAR imaging, a long image integration time is required to produce fine image resolution. However, a long image integration time does not always guarantee good cross-range resolution. This is illustrated in the discussion above where it is found that the amount of blurring caused by non-uniform target motion over the imaging period can be quite severe.

Time-frequency techniques have been used to "refocus" blurred ISAR images [5]. As seen from the discussion above, the blurring of ISAR images is a consequence of a time-varying Doppler frequency resulting from non-uniform motion of the target. By extracting an ISAR image of the target at a particular instant of time, a better-focused image can be obtained because the target's motion can be considered as relatively uniform over a short duration. However, there will be a large number of time instants to deal with in most time-frequency processing. Thus, a large number of refocused ISAR images will emerge, corresponding to the number of time instances. For fast, efficient target recognition, it is desirable to make use of only the best refocused image. It is impractical to examine all available refocused ISAR images. Visual inspection manually over a large number of images, or even using an automated image search algorithm only adds complexity to the target recognition process.

A more efficient way to determine the optimum refocused ISAR image is possible, based on the insights obtained from the image distortion analysis conducted above. That is to say, it is found from the experimental and numerical analyses that the blurring is directly related to the amount of change in the Doppler frequency of the target during the imaging duration. This fact is used in the refocusing process. Figure 13 shows another distorted ISAR image of the TMS target. This image is chosen for its varied Doppler frequency over the imaging period. The corresponding temporal Doppler history of the target is shown in Figure 14.

Before discussing how an optimum refocused ISAR image can be determined, it is useful to take a look at samples of the refocused images at various time instants. A refocused ISAR image is reconstructed from the spectrograms of all the down-range bins of the distorted ISAR image at a chosen time instant. The spectrogram is computed using Short Time Fourier Transform (STFT) with a 0.4 s image integration time window. This is illustrated by the duration T in Figure 14. In other words, each time instant represents a 0.4s time segment. Thus it is more accurate to describe a time instant as a short duration of time rather than a precise point in time. Figure 15 shows the refocused ISAR images of the target at 6 time instants as indicated in Figure 14. The ISAR image at time t_a corresponds to the instance when the target has an uniform rotational motion. This image serves as a reference image for comparing with the refocused images at other time instances. Using a 0.4s STFT, the resolution is just barely adequate to resolve the scatterers on the target in the cross-range direction for the uniform rotation case at t_a. A quick inspection of Figure 15 reveals that the best refocused image is at the time instance t_e and the worst images are at t_c, t_d and t_f.

By understanding why the images are the worst at t_c and t_d and why the image is the best at t_e, we can develop an objective methodology on how to reconstruct the optimum refocused ISAR image. The ISAR image at t_c appears compressed. This is due to the small Doppler frequency (i.e., small angular rotational rate) of the target at this time instant. It is even smaller than the uniform rotation case at t_a; this is illustrated in Figure 14. The Doppler motion is too small to separate the scatterers adequately in the cross-range direction. The ISAR images at time t_d and t_f still appear blurry, with some of the scatterers still not properly focused. This is attributed to the fact that the Doppler motion of the target is going through a large temporal rate of change within these time instants, i.e., $\Delta f / \Delta t$ is large.

The ISAR image at t_e has all six scatterers on the target clearly resolved and provides the best-refocused image. There are two reasons why the best image quality is found at time instance t_e. Firstly, the Doppler motion is large, significantly larger than the uniform rotational rate case at the time instant t_a (see Figure 14). Hence the scatterers are much better separated by the large angular rotational rate in the cross-range. Secondly, the temporal rate of change of the Doppler motion in the time interval at t_e is small; i.e., $f/\Delta t$ is small. Therefore, the blurring to the image of the scatterer is kept to a minimum. The STFT window T for time instant t_e is indicated in Figure 14. It can be seen that the Doppler motion varies very little within time instant t_e.

Based on the analysis of the refocused images shown in Figure 15, we have deduced a few simple physical rules that will enable us to extract a relatively well focused image from a blurred ISAR image:

1. From the blurred image, locate a down-range bin where it contains the most severe blurring in the cross-range.

2. Produce a time-frequency spectrogram at the chosen down-range bin, using Short-Time Fourier transform or time-frequency distribution functions [6].

3. From the spectrogram, select a time instance when the variation of the Doppler motion is small (i.e., small $f/\Delta t$) and the value of the Doppler motion is large (i.e., as far away from the zero Doppler frequency as possible).

4. Construct spectrograms at all down-range bins from the blurred ISAR image that contain the target. Recombine the same time instance from all spectrograms to reconstruct a focused ISAR image.

This procedure provides a much faster means of constructing an optimum refocused image. This is because once the appropriate time instance is determined, only one ISAR image needs to be reconstructed. This is obviously much more efficient than extracting ISAR images at all time instances from all spectrograms because the number of time instances is usually very large. Another interesting note is that having a large amount of blurring in the ISAR image may actually be better than having just a small amount of blurring for restoring a focused image. A more severe blurring means that at some time instant, there is a large Doppler motion that can be exploited to get a better-resolved image.

6.0 CONCLUSIONS

From the results of the numerical analysis and the comparison with experimental data, it can be concluded that phase modulation effect can be modelled properly by including the temporal variation of the target's motion in its angular rotational rate. That is to say, the angular rotational velocity must be described as a function of time; i.e.,$\omega(t)$ so that an instantaneous Doppler velocity can be ascribed at any given time. The conventional quadratic phase distortion is shown to be a special case of phase modulation and it is a second order effect. The quadratic phase distortion is much smaller than that from phase modulation where a target displaces only a few degrees in angular rotation during the ISAR imaging period. The distorted image can be refocused using time-frequency analysis methods. An efficient procedure to find the best refocused image from a severely blurred image has been developed and demonstrated.

7.0 REFERENCES

[1] T. Sparr, S-E. Hamran and E. Korsbakken, "estimation and Correction of Complex Target Motion Effects in Inverse Synthetic Aperture Imaging of Aircraft", IEEE Radar 2000 Conference, pp.457-462, USA, May 2000.

[2] V. C. Chen and W. J. Miceli, "Simulation of ISAR imaging of moving target", IEE Proc. – Radar, Sonar and Navigation, Vol. 148, No.3, pp160-166, June 2001.

[3] D. Wehner, "High Resolution Radar", Artech House, Boston, 1987.

[4] S. K. Wong, G. Duff and E. Riseborough, "Distortion in the inverse synthetic aperture radar (ISAR) images of a target with time-varying perturbed motion", IEE Proc. Radar, Sonar and navigation, Vol.150, No.4, pp.221-227, August 2003.

[5] V. C. Chen and H. Ling, "Time-Frequency Transform for Radar Imagery and Signal Analysis", Artech House, Boston, 2002.

[6] Leon Cohen, "Time-Frequency Distributions – A Review"; Proceedings of the IEEE, Vol.77, No.7, pp.941-980, July 1989.

ACKNOWLEDGEMENTS

Financial support by Dr. William Miceli of the US Office of Naval Research–International Field Office under the NICOP program is gratefully acknowledged.

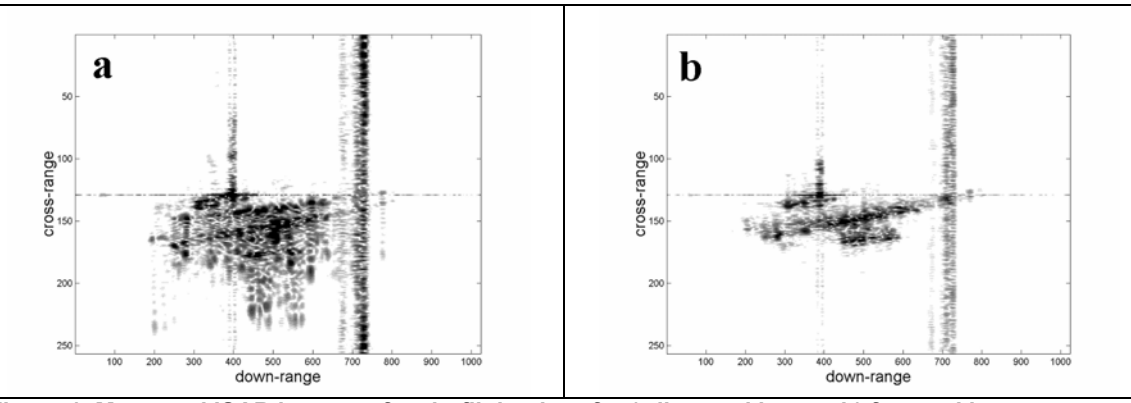

Figure 1 Measured ISAR images of an in-flight aircraft. a) distorted image, b) focused image.

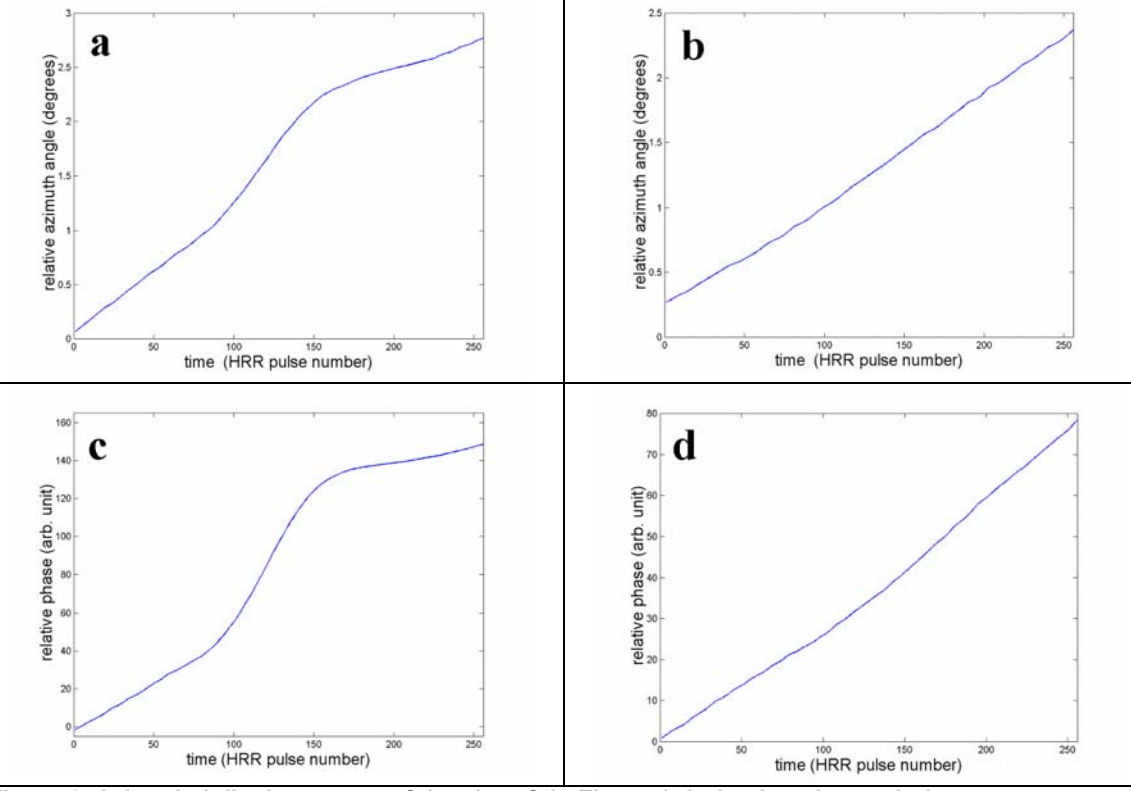

Figure 2 Azimuthal displacements of the aircraft in Figure 1 during imaging period:
a) distorted image, b) focused image.
Temporal phase history of a scattering centre on the aircraft: c) distorted image, d) focused image.

Figure 3 The Target Motion Simulator (TMS) experimental apparatus.

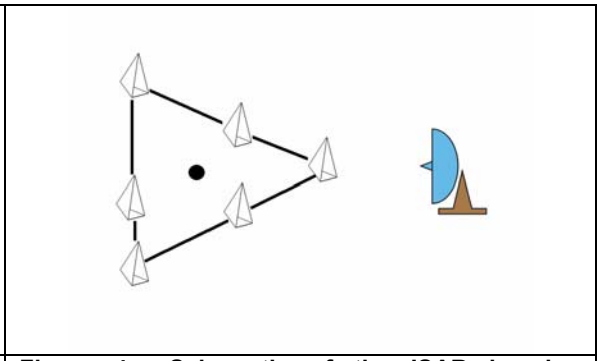

Figure 4 Schematic of the ISAR imaging experimental set-up.

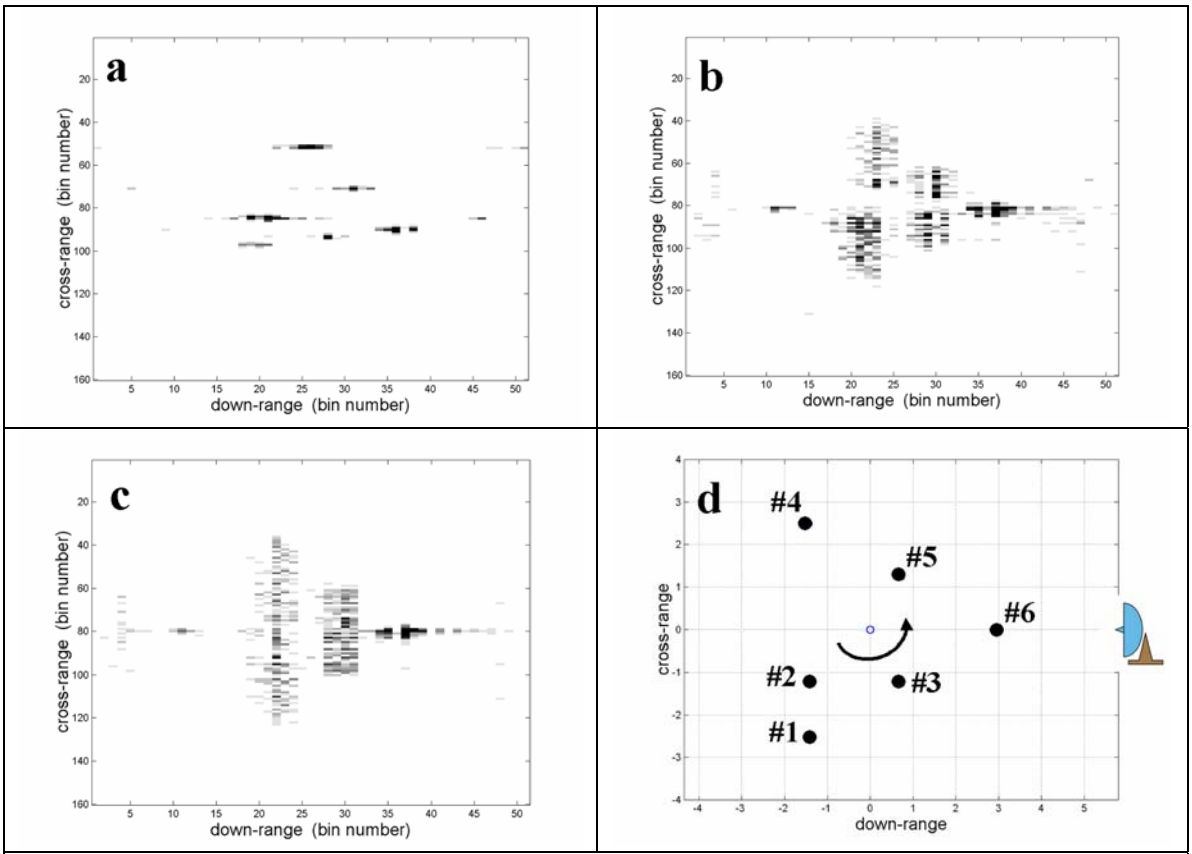

Figure 5 A sequence of measured ISAR images of the TMS target. a) constant rotation at 2 degrees/s, b) oscillating motion introduced to the target's rotating motion, c) target with oscillating motion at a later time, d) the TMS target's orientation with respect to the radar for ISAR image in c). The target is rotated in the counter-clockwise direction.

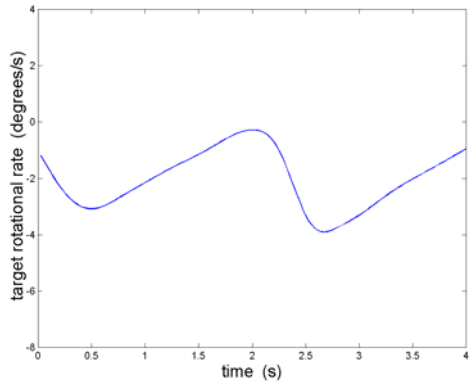

Figure 6 Measured temporal motion of the Target Motion Simulator.

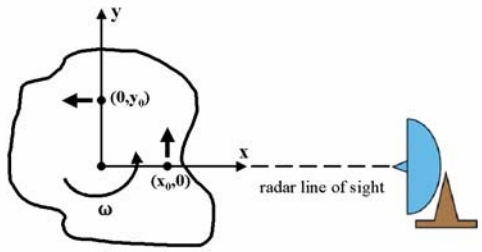

Figure 7 Schematic of a rotating target with examples of two scattering centres illustrated.

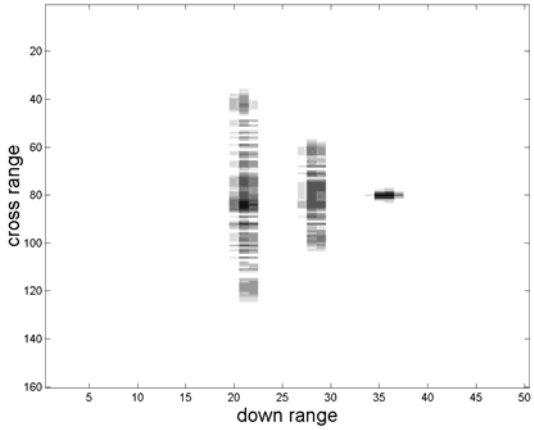

Figure 8 Computed distortion in the ISAR image using the phase modulation model. See and compare with the experimental image in Figure 5c.

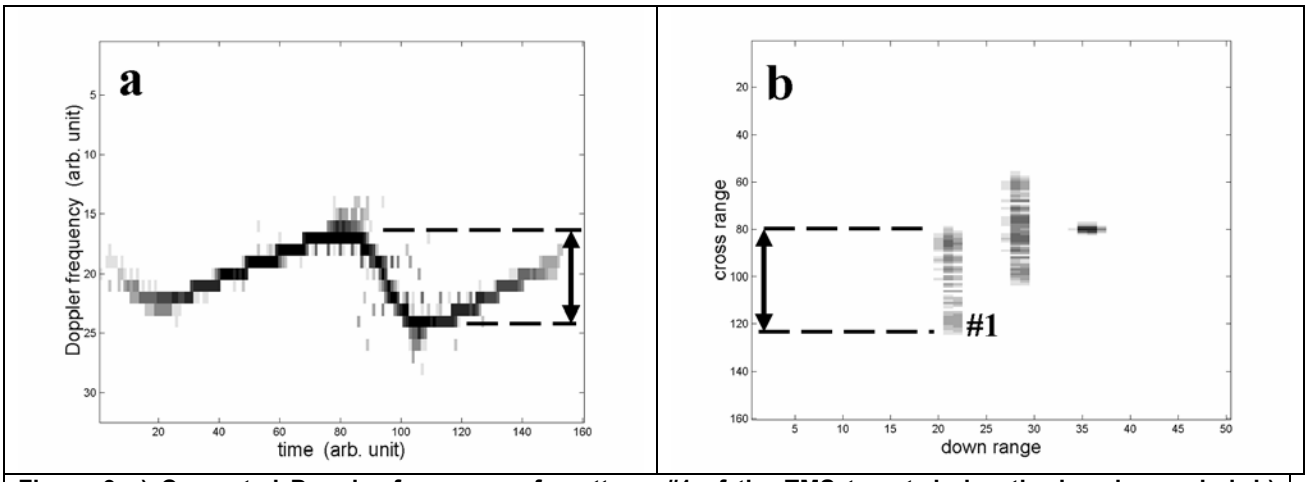

Figure 9 a) Computed Doppler frequency of scatterer #1 of the TMS target during the imaging period, b) Computed ISAR image of the TMS target with scatterers #2 and #4 removed in the computation. The amount of distortion of scatterer #1 corresponds to the amount of change in the Doppler frequency.

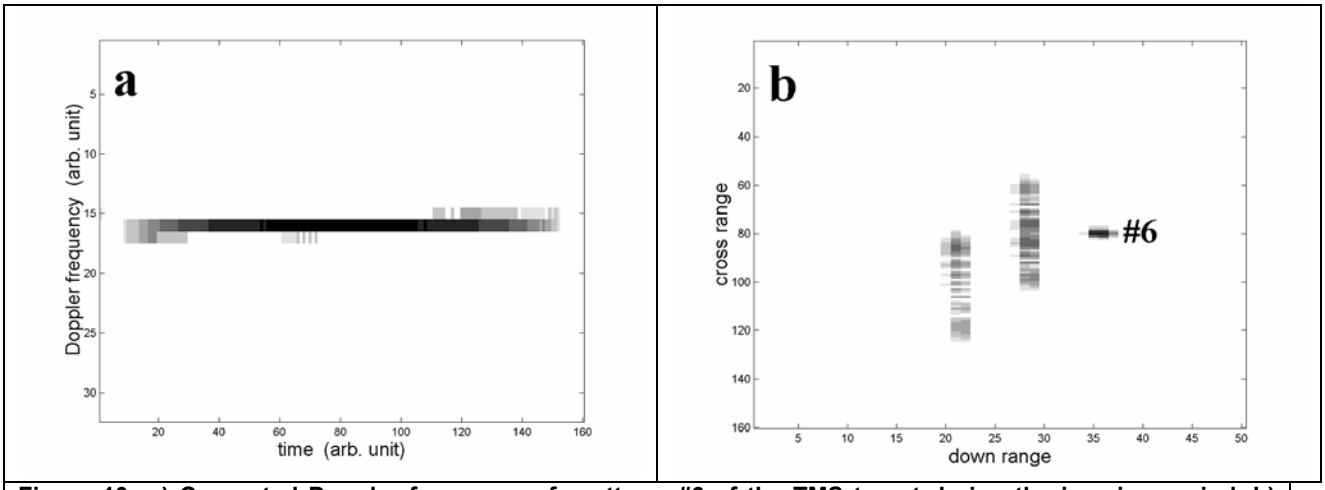

Figure 10 a) Computed Doppler frequency of scatterer #6 of the TMS target during the imaging period, b) Computed ISAR image of the TMS target with scatterers #2 and #4 removed in the computation. The amount of distortion of scatterer #6 corresponds to the amount of change in the Doppler frequency.

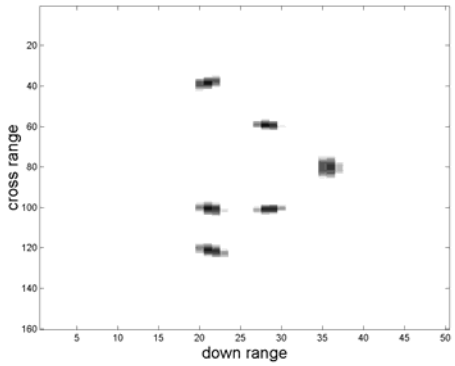

Figure 11 ISAR image of the TMS target using a constant rotational rate of 3.9 degrees/s.

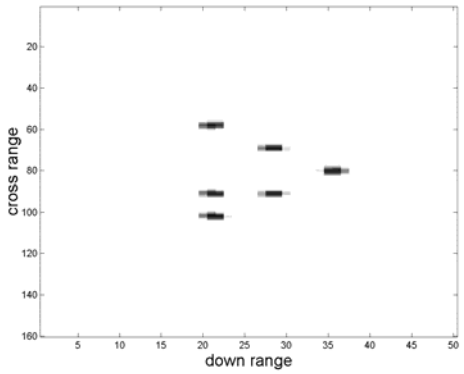

Figure 12 ISAR image of the TMS target using a constant rotational rate of 2 degrees/s.

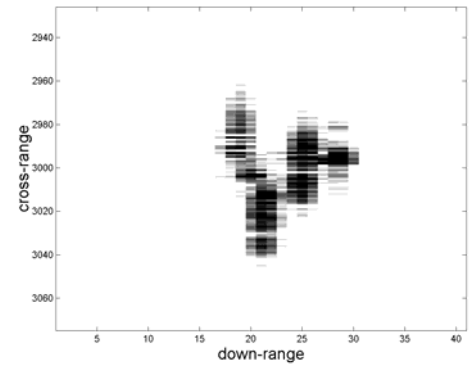

Figure 13 Distorted ISAR image of the TMS target (experimental).

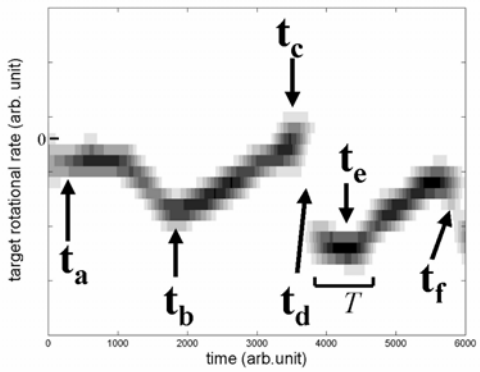

Figure 14 The temporal motion of the target corresponding to the distorted ISAR image in Figure 13. T is the STFT duration.

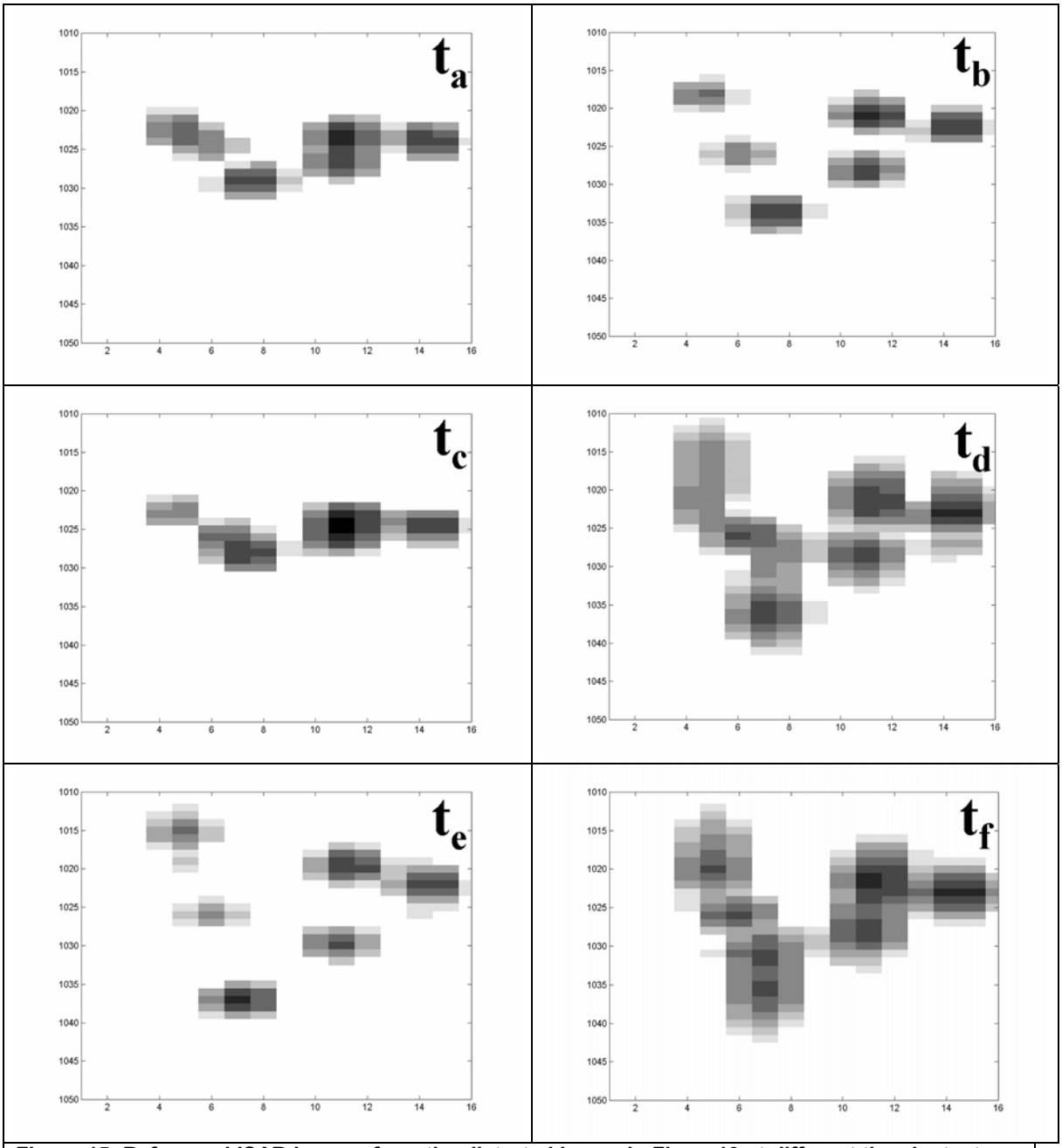

Figure 15 Refocused ISAR images from the distorted image in Figure13 at different time instants as indicated in Figure 14.